A CONTRIBUTION TO THE OPTIMAL DESIGN OF RIDE-RINGS FOR INDUSTRIAL ROTARY KILNS

by

Heng Long Li
Graduate Student

and

Panos Papalambros
Assistant Professor

Department of Mechanical Engineering
and Applied Mechanics
The University of Michigan
Ann Arbor, MI 48109-2125

April 1982

Revised
February 1984

ABSTRACT

The design of the ride-rings, or tyres, of industrial rotary kilns is studied as a nonlinear programming problem. The method of monotonicity analysis is employed to obtain results of sufficient generality and utility to the designer. A special-purpose algorithm for the location of the global optimum is presented. A parametric study provides design charts showing the range of criticallity for the various design requirements.

The article represents the type of modeling analysis and subsequent solution, suitable for design problems which must be solved many times with parameter changes larger than those handled with the usual sensitivity analysis.

INTRODUCTION

Rotary kilns are widely used in the processing industries, such as cement, ore-processing and chemical. The kiln (Fig. 1) consists of a cylindrical shell slightly inclined from the horizontal position and supported by ride-rings (often called also tyres) riding on pairs of rollers. A gear rim and pinion assembly rotates the entire system. Material enters the kiln at the upper end and moves towards the lower end, with continuous mixing and a supply of hot air. The desired chemical reaction is completed at the lower end and thus the processing is continuous. The kiln shell has a firebrick lining to protect the steel outer shell from the high temperatures existing inside. The ride-ring is a cylindrical steel tyre connected to the shell and rotating with it.

Economies of scale in the cement and ore-processing industries have led to manufacturing of large-diameter units resulting to loads of several hundred tons carried by the ride-rings. The rings themselves weight several tens of tons. As units become larger, it is important to review existing practices and determine rationally the proper selection of design quantities so that maximum efficiency and minimum cost may be achieved. As a contribution towards this goal, the present article examines the rational design of a key component of the rotary kiln system, i.e. the ride-ring, or tyre. The approach used is to formulate a simple mathematical model of the design as a nonlinear programming problem.

The design, manufacturing and operation of rotary kilns is a mature subject. However, new analysis and computational tools are finding increasingly more use, as evidenced by recent literature primarily of European and Japanese sources [1 - 11].

Other equipment similar to rotary kilns such as rotary coolers and drum dryers, is designed under the same principles. However, the heat load is lower and the dimensions are usually smaller.

The ride-ring is an important component of the kiln system. Theoretical and experimental investigation of shell deformations using special instruments ("Shell tester" [1, 2]) shows that the greatest shell deformation occurs in the vicinity of the ride-rings, so that rigidity of the structure at those points is an important consideration. Surface contact and bending stresses are also important and influence the design of the shell and the supporting system. In traditional design procedures one of these criteria, usually the contact stress, is selected to be met fully by the design. Thus material capabilities may not be fully utilized.

The present article poses the ride-ring design as an optimization problem, the formulation being derived first. Then the model is analyzed using the principles of monotonicity analysis [13-19]. This method is chosen because the results can be used to derive easily engineering insights about the optimum. Iterative optimization methods, e.g. penalty functions (SUMT) and sequential quadratic programming (VMCON), were used and found in agreement with the results presented here; however, their repeated application is tedious and the numerical answers not globally conclusive, so no further consideration is given to these methods here. Numerical examples and parametric analysis of the optimal solution follows the optimization analysis.

A computer program is described and design charts are included. Thus the method presented can be used as a general design procedure for any ride-ring with customary cross-sectional shape and a variety of specifications.

The present optimization study of the ride-ring is part of a larger study of the entire rotary kiln design which will be reported in a subsequent article.

PROBLEM FORMULATION

The purpose of the present analysis is to provide some understanding of the appropriate selection of design variables in the preliminary design stage. The ride-ring design is modelled as a nonlinear programming (NLP) problem. The model is kept quite simple, and liberal use of design experience is included in order to account for design requirements that require substantial modeling effort. This allows the identification of global solutions to the optimization problem.

The overall manufacturing cost of the ride-ring can be considered as an increasing function of the weight, so minimum weight is chosen as the objective of the NLP problem. The constraint set includes contact and bending stresses limited by the fatigue strength of the material, and deformations limited by possible damage to the shell's brick lining. System requirements such as production rate, kiln length and support spacing essentially determine the size of the inner diameter of the ring. Therefore, it is the cross-section of the ring that must be specified in the preliminary design, the ring being viewed as a component of the system. Two configurations of cross-section will be examined, as most common: rectangular and box type. This section describes the formulation of the NLP model. The Nomenclature includes explanation of the symbols used.

Weight and Geometry of Cross-Section

For large ride-rings, a solid rectangular cross-section (Fig. 2 a) is used, primarily for easy manufacturing. The weight of the ring is then

$$G_r = 2\pi g\, r_c\, b_r\, h \qquad (1)$$

where

$$r_c = (D_p+h)/2 \qquad (2)$$

For smaller ride-rings, a box-type cross-section is used sometimes (Fig. 2 b), for a lighter but rigid construction.

The meridional symmetry of the cross-section suggests that it may be decomposed into three significant parts so that the original section can be compacted into an equivalent I section, as in Fig. 3. Using the equivalent I section simplifies the analytical expressions of the section properties. Thus the weight may be expressed as

$$G_r = 2\pi g r_c a_r + 0.5gNd_2(h-d_2-2.0)(b_r-a) \quad (3)$$

where

$$a_r = ah + (b-a)d_1 + (b_r-a)d_2 \quad (4)$$

$$a = d_1 + d_2 \quad (5)$$

In (3), the second term represents weight of flanges with thickness $0.5d_2$ and N is an integer usually close to $\pi d_r/60$. The centroid location is given by

$$c_1 = [ah^2+(b-a)d_1^2 + (b_r-a)d_2(2h-d_2)]/2a_r \quad (6)$$

$$c_2 = h-c_1 \quad (7)$$

$$r_c = D_p/2 + c_1 \quad (8)$$

Since the outer surface is subjected to wear, we should select $d_2>d_1$; it is usually suggested that

$$d_1 = 0.65d_2 \quad (9)$$

and this relationship will be assumed here.

Thus, for the rectangular cross-section, the design variables are simply h and b_r, while for the box-type, d_2 and b must be added also.

Stress Constraints

The service life of the ride-ring is usually taken as 20 years and the speed of rotation is in the range of 0.5 - 3.0 rpm, depending on the working conditions. Thus cyclically stressed parts are considered under fatigue conditions for a total 10^8 cycles [12].

The outer fibers of the ring experience contact Hertz stresses at the contact areas of the ring and the supporting two rollers. Considering the case of two cylinders in parellel-axis contact (Fig. 4a) the contact stress constraint is expressed as [20]

$$\sigma_H = 1.869[E(Q+G_r)(1.732b_r)^{-1}(d_r+D_t)/d_rD_t]^{1/2} \leq \sigma_{HW} \quad (10)$$

where

$$d_r = D_p + 2h \quad (11)$$

and σ_{HW} is the working stress of the material. Experience in design and maintenance of rings indicates that σ_{HW} is limited within a narrow range near 400 MPa for medium-carbon structural steels, in which fatigue and wear are considered together.

Note that the diameter of the roller, D_t, is selected through an appropriate ratio r of the outer ring diameter d_r to D_t. Usually r is taken in the range 3.0 - 3.8, while D_t must be a standard size as 1.0, 1.1, 1.2, 1.4, 1.6, 1.8, 2.0,... (meters). But with the inner diameter of the ride-ring known, D_t can be treated as known, too.

The load of the kiln shell is transmitted to the ring through the base plates welded on the outer surface of the shell (Fig. 4b). There are about 20-40 base plates (washers) per ring so that the pressure distribution on the ring can be considered approximately as a continuous cosine function (Fig. 5a). At the top, there is always some clearance Δ between ring and plates, so no pressure is exerted on the ring within the initial angle α_o. Thus, the pressure on the inner ring fibers is given by $q = q_o (\cos \alpha_o - \cos \phi)$, where

$$q_o = (Q+G_r)/r_c(\pi-\alpha_o+0.5\sin 2\alpha_o) \quad N/cm \quad (12)$$

The calculation of bending moment distribution is a statically indeterminate problem. Detailed analysis, using e.g. Castigliano's Theorem, shows that the maximum moment occurs in the contact areas (Fig. 5b) and depend on the initial angle α_o as shown below:

TABLE 1: Maximum Bending Moment Versus Initial Angle

α_o	0°	30°	45°	60°	90°
$M_{max}/(Q+G_r)r_c$	0.0861	0.0847	0.0819	0.0773	0.0629

For the worst case, at $\alpha_o = 0$ and no clearance between base plates and ring (which never occurs in practice) we take the conservative estimate

$$M_{max} = 0.0861\ (Q+G_r)r_c \tag{13}$$

Now the bending stress constraint is expressed as

$$\sigma_B = 10M_{max}/w \leq \sigma_{BW} \tag{14}$$

where

$$w = b_r h^2/\sigma \tag{15}$$

for rectangular section, while for box section where $c_1 > c_2$ as a consequence of $d_2 > d_1$, we have

$$w = i_r/c_1 \tag{16}$$

with

$$i_r = [bc_1^3-(b-a)h_1^3+b_r c_2^3-(b_r-a)h_2^3]/3 \tag{17}$$

$$h_1 = c_1-d_1\ ,\quad h_2 = c_2-d_2 \tag{18,19}$$

Temperature Effects

The working temperature inside the kiln is in the range of 1000-1500 °C, the shell temperature is around 300°C and an average temperature of the ride-ring is about 100°C. Thermal stresses may arise due to the following reasons:

(i) Temperature gradients between inner and outer fibers. A temperature difference of 30°C or higher may be expected with resulting tensile stresses uniformly distributed around the circumference. This assumes no temperature variations on the shell itself due to uneven hot material distribution inside. The allowable stresses chosen in (10) and (14) take this effect into account.

(ii) Too small mounting clearances between shell and ring. Uniform tensile stresses result again. This is generally avoided by proper design.

(iii) Excessive heat transfer from the ring to the rollers. This would result in fluctuating normal stresses essentially in-phase with the contact stresses [1,21,22]. Detailed analysis is not considered necessary for preliminary design and this effect is included in the value of σ_{HW} in (10).

Deformation Constraints

An important design consideration is the radial deformation of the ring. The stiffness of the ring is considerably larger than that of the relatively thin shell. Near the support area, it can be assumed that, the kiln shell deformation is nearly the same as that of the ring. During rotation, deformations will follow a pattern similar to the bending stress distribution curve in Fig. 5b. Thus the firebrick wall inside the shell will be damaged, with eventual collapse and interruption of the kiln operation.

A measure of this deformation is given by the ellipticity defined as the difference between the largest and smallest diameter after loading. This ellipticity must be limited to appropriate values. Deflections are derived in a similar manner as the stresses. Due to symmetry, only top, bottom, and horizontal points need be analyzed. The resulting deformation constraint may be expressed as

$$e = 0.814(Q+G_r)r_c^3/Ei_r \leq e_w \qquad (20)$$

In a final note, it should be mentioned that finite element analysis has been used to prove that the above stress and deformation analytical expressions are fundamentally correct and their simplicity makes them appropriate for design purposes.

The model is completed by including dimensional limits for the box-type section:

$$0.8b_r \leq b \leq 1.1b_r \quad , \quad 0.28h \leq d_2 \qquad (21,22)$$

Clearly, $h < D_p/2$ since D_p is large. In addition, limitations such as $1.65d_2 \leq h$, $h-d_2-2.0 \geq 0$, $b_r-a \geq 0$, $b-a \geq 0$, and so on, could be included. However, interesting designs should not have these constraints active, as design experience indeed shows, and therefore such limitations are excluded from the model.

OPTIMIZATION ANALYSIS

This section describes the solution of two nonlinear programming problems, one for rectangular and another for box type cross-sections. All intermediate variables and most equality constraints are eliminated. Thus the first problem results to three inequality constraints and two design variables, while the second has 10 constraints and seven variables. Lack of evident convexity suggests caution in the use of numerical iterative methods, while the nonlinearities present discourage classical analytical methods. Therefore, the problems are treated by monotonicity analysis first, in order to identify the active (i.e. critical) constraints and reduce the size of the problem [13-19] to the point where a global solution can be identified. The method is adequately described in the references and is applied here directly.

Rectangular Solid Cross-Section

Assembling the results of the previous section we formulate the following nonlinear programming statement

Problem 1

minimize

$$G_r = \pi g b_r h (D_p+h) \tag{23}$$

subject to

$$R_1: \quad \frac{1.869}{\sigma_{HW}} \left\{ \frac{(Q+\pi g (D_p+h) b_r h) E}{1.732 b_r} \left(\frac{1}{D_t} + \frac{1}{D_p+2h} \right) \right\}^{1/2} \leq 1$$

$$R_2: \quad 2.583 (Q+\pi g (D_p+h) b_r h) (D_p+h) / b_r h^2 \sigma_{BW} \leq 1$$

$$R_3: \quad 1.221 (Q+\pi g (D_p+h) b_r h) (D_p+h)^3 / E b_r h^3 e_W \leq 1$$

The design variables are b_r, h and the remaining quantities are the design parameters, i.e. constants for the model and inputs for the problem. Constraints R_1, R_2, R_3 represent contact stress, bending stress and deformation limits respectively.

We start the analysis by observing that constraint R_1 alone cannot be active, because the objective requires lower

bounds on both b_r and h, while R_1 provides a lower bound on b_r but an upper bound on h. Therefore, the problem is bounded only if at least one of R_2, R_3 is also active. Thus, without any assumption on activity for R_1 we should examine under what conditions R_2 or R_3 can be active. To this end, we define

$$u \triangleq (Q+\pi g(D_p+h)b_r h)(D_p+h)(b_r h^2)^{-1} \tag{24}$$

so that constraints R_2, R_3 can be rewritten as

$$R_2: \quad u \leq (1/2.583)\sigma_{BW} \equiv u_2 \tag{25}$$

$$R_3: \quad u \leq (1/1.221)Ehe_w(D_p+h)^{-2} \equiv u_3 \tag{26}$$

Now we observe that if $u_2 \neq u_3$ at the optimum, then either R_2 or R_3 will be redundant and so non-critical. Letting $u_2 = u_3$ and rearranging, we get

$$h^2-2(A_1-D_p)h+D_p^2 = 0 \tag{27}$$

where

$$A_1 \triangleq 1.0577\ Ee_w\sigma_{BW}^{-1} \tag{28}$$

The solution of the guadratic in h equation (27) is

$$h_1,h_2 = (A_1-D_p) \pm ((A_1-D_p)^2-D_p^2)^{1/2} \tag{29}$$

with h_1,h_2 being the smaller, larger respectively roots. Since for reasonable choices of parameters, $A_1 >> D_p$, both h_1 and h_2 will be real, positive and one of them much larger than D_p. Thus we conclude that the following possibilities may occur:
(A) For $h_1<h<h_2$ ($u_2<u_3$), constraint R_2 is critical and R_3 is non-critical.
(B) For $0<h\leq h_1$ ($u_2\geq u_3$), constraint R_3 is critical and R_2 is redundant (in the equal case, R_2 and R_3 are equivalent)
(C) For $h\geq h_2$, no possible solution exists and this case can be omitted.

The above result is in agreement with an intuitive understanding of the trade-offs between bending and deformation limitations: if e_w is (relatively) large and σ_{BW} is small, then bending stress limitations are more important than deformation limitations and the value of A_1, eq.(28), is large while

h_1 is small; the optimum will result in case A with bending stress constraint R_2 being critical. Similarly for the case B.

Further analysis in both cases A and B shows that for a bounded problem, constraint R_1 must be also active. Thus the global optimum is found by solving the systems of equations ($R_1 = 1$, $R_2 = 1$) and ($R_1 = 1$, $R_3 = 1$) for h and b_r and then comparing the corresponding values of the objective G_r. Usually only one of the cases is feasible. In summary, the solutions are obtained as follows:

Case A: Solve the cubic equation for h_A:

$$2C_A h_A^3 + (C_A(D_t+D_p)-2)h_A^2-3D_p h_A-D_p^2 = 0 \qquad (36)$$

where

$$C_A = 0.7807ED_t^{-1}\sigma_{HW}^{-2}\sigma_{BW} \qquad (37)$$

and admissible values in the range $h_1<h_A<h_2$.

Case B: Solve the quartic equation for h_B:

$$2(C_B-1)h_B^4 + (C_B(D_t+D_p)-7D_p)h_B^3-9D_p^2h_B^2-5D_p^3h_B-D_p^4 = 0 \qquad (38)$$

where

$$C_B = 1.652E^2D_t^{-1}e_W\,\sigma_{HW}^{-2} \qquad (39)$$

and admissible values in the range $0<h_B\leq h_1$.

The identification of active constraint R_1 in both cases allows the use of a single expression for the calculation of the optimal b_r, ie.

$$b_r = Q^{-1}\left\{\frac{4.9596^2\,HW}{E(D_t^{-1}+(D_p+2h)^{-1})} - \pi gh(D_p+h)\right\} \qquad (40)$$

where h is equal to h_A or h_B for case A or B respectively.

It should be noted that the above analysis is an example of regional monotonicity [15].

Numerical Example: Given parametric values

$$D_p = 264.4\text{cm},\ D_t = 100\text{cm},\ Q = 883\text{kN},\ g = 0.0765\text{N/cm}^3$$

$$E = 19.6(10^4)\text{MPa},\ e_W = 0.5\text{cm},\ \sigma_{HW} = 392.4\text{MPa},$$

$$\sigma_{BW} = 49\text{MPa} \tag{41}$$

we calculate $A_1 = 2115$, $h_1 = 18.98$cm, $h_2 = 3683$cm. For case A, solving (36) we get $h_A = 21.0$cm in the acceptable range. From (40) and (23) we get $b_r = 31.65$cm and $G_r = 45.6$ kN. For case B, solving (39) we get $h_B = 20.3$cm which is outside the interval $(o,h_1]$, so this case is discarded. Thus, the global optimum is $(b_r^*, h^*) = (31.7, 21.0)$.

Box Type Cross-Section

The nonlinear programming statement for this problem is

Problem 2

minimize G_r (42)

subject to

$$R_1 = \left\{2\pi g(0.5D_p+c_1)a_r+0.5gNd_2(h-d_2-2)(b_r-1.65d_2)\right\}G_r^{-1} = 1$$

$$R_2 = (1.65h+0.65b+b_r-2.7225d_2)d_2a_r^{-1} = 1$$

$$R_3 = (1.65h^2+0.4225bd_2+2hb_r-1.3d_2h-b_rd_2-0.0471d_2^2)d_2(2c_1a_r)^{-1} = 1$$

$$R_4 = 2.017E(Q+G_r)(D_t^{-1}+(D_p+2h)^{-1})b_r^{-1}\sigma_{HW}^{-2} \leq 1$$

$$R_5 = 0.861(Q+G_r)(0.5D_p+c_1)c_1i_r^{-1}\sigma_{BW}^{-1} \leq 1$$

$$R_6 = \left\{bc_1^3-(b-1.65d_2)(c_1-0.65d_2)^3+b_r(h-c_1)^3-(b_r-1.65d_2)(h-c_1-d_2)^3\right\}(3i_r)^{-1} = 1$$

$$R_7 = 0.814(Q+G_r)(0.5D_p+c_1)^3(Ee_wi_r)^{-1} \leq 1$$

$$R_8 = 0.8b_rb^{-1} \leq 1$$

$$R_9 = 0.909\ bb_r^{-1} \leq 1$$

$$R_{10} = 0.28\ hd_2^{-1} \leq 1$$

The design variables are b, b_r, d_2, h; G_r, a_r, c_1, i_r, the last four considered as intermediate variables defined by the equality constraints R_1, R_2, R_3 and R_6 respectively. The remaining quantities are considered constant. Constraints R_4, R_5, R_7 express contact

stress, bending stress and deformation limitations respectively, while R_8, R_9 and R_{10} are the dimensional limits (21) and (22). This latter set of constraints express practical limitations resulting from design experience and need not be satisfied in a strict sense. In the optimization analysis they can be considered non-critical a priori and an optimum design should be sought initially under the physical limitations of R_4, R_5 and R_7 The optimum solution thus obtained, if it exists, should be checked against the practical limitations. If any of the practical constraints is violated, the designer may choose to include it in the model at this point and reexamine the location of the new optimum. In this case, the new optimum will be in fact limited by the model itself and further examination of the model may be necessary in order to elucidate physical or economic limitations not previously included.

To simplify matters, we observe that the weight G_r is usually 5-8% of the design load Q, so the term $Q+G_r$ appearing in R_4,R_5 and R_7 is substituted by the term 1.07Q without significant loss of accuracy. Furthermore, since usually $h << D_p$ we also have $c_1-h/2 << h$, so we can approximately set $r_c = 0.5D_p+C_1 \approx 0.5(D_p+h) = r_c(h^+)$ and take $c_1 = c_1(h^+)$, but only for the purpose of monotonicity analysis.

With the previous observations taken into account, we arrive at the following expression of the problem in terms of functional monotonicities,

minimize

$$G_r = G_r(b_r^+, h^+, b^+, d_2^+)$$

subject to

$$\begin{aligned} R_4(b_r^-, h^-) &\leq 1 \\ R_5(b_r^-, h, b^-, d_2) &\leq 1 \\ R_7(b_r^-, h, b^-, d_2) &\leq 1 \end{aligned} \tag{43}$$

where the equality constraints were used to eliminate the variables G_r, a_r, c_1 and i_r, and the practical constraints

are (temporarily) ignored.

In a similar manner as in Problem 1, we can find two cases:

(A) For $C_1<c_1<C_2$, R_5 is critical and R_7 non-critical

(b) For $0<c_1\leq C_1$, R_7 is critical and R_5 non-critical.

where

$$C_1,\ C_2 = 0.5\left\{(A_1-D_p) \pm ((A_1-D_p)^2-D_p^2)^{1/2}\right\} \qquad (44)$$

with C_1, C_2 being the smaller, larger root respectively. From (43) follows that one of these two constraints must be active in order to bound the variable b. Using implicit elimination of variables and applying the implicit function theorem for monotone functions [17] it can be shown that, as in Problem 1, in both cases constraint R_4 must be active. Thus, both cases are reduced to a problem with two degrees of freedom, i.e. four variables and two active constraints. This problem is quite complicated so it must be solved numerically with an appropriate search method.

Based on the above analysis, a computer program is written for the box type problem. The flow chart is given in Fig. 6. Cases A and B are represented by I = 1, I = 2 respectively. Decision variables are h, d_2 and state variables are b, b_r, thus chosen for convenience of solution. The variables h and d_2 take discrete values at 5mm intervals, so a general purpose NLP code is not appropriate. Instead, since the search range for h and d_2 is quite narrow, an exhaustive search with very limited number of steps is utilized. This search is so inexpensive that no additional effort is justified for using a more elaborate method, such as a Fibonacci search. The practical constraints are included as well. The program was run for several cases and converged rapidly. Some results will be discussed in the next section. It should be noted that the original problem was also solved using iterative algorithms that required significantly more computational effort, and in some cases no convergence was achieved.

DESIGN RESULTS

From the preceding analysis, it is evident that the procedure can be applied for any set of specified parameters. It is interesting to investigate in what ranges of parameters we may have criticallity of bending versus deformation. As shown earlier, the contact stress constraint is always critical which, in fact, justifies formally the traditional design procedure. Moreover, the value of the contact working stress will have an inverse effect on the weight. Different combinations of the bending working stress and working deformation will lead to either of cases A and B. This event is represented by two regions in Figures 7 and 8. These figures correspond to solid and box type cross sections and show the location of the optimum design influenced by changes in the bending and deformation limits.

The two regions in the above figures emphasize the trade-offs between the bending stress and deformation limitations. Changes in σ_{HW} would move the dividing line only slightly (Fig. 7). In each region, the weight is affected by <u>only one</u> of σ_{BW} and e_W. For example, if emphasis is put on a small deformation e_W in order to keep good stability of the firebrick walls, any attempt for improvement in material quality for bending load carrying capacity is unnecessary, yielding no further improvement in weight reduction. In contrast, for other applications without firebrick lining, such as coolers and dryers, a relatively large e_W is allowed so that improvements in bending load carrying capacity will reduce the weight of the ring.

CONCLUSION

A nonlinear programming formulation with minimum weight objective was used for the ride-ring design problem. The method of monotonicity analysis was used successfully to investigate the criticallity of constraints and location of the optimum.

The contact stress constraint was found always active confirming the "full contact stress" design procedures in use. Bending stress and deformation constraints may be active, depending on the application, and the range of their relative importance was established. However, only one of them need be used for weight reduction.

The location of the optimum is obtained globally with a special-purpose algorithm that does not employ a descent scheme but an exhaustive search in a very narrow range of standard values of the design variables. Thus, efficiency and reliability are guaranteed, which may not be achieved with a general-purpose iterative method.

The design investigation is currently being pursued further by studying the design of the shell, rollers and drive in addition to the ride-ring and formulating a system optimization model that includes more components of the kiln.

ACKNOWLEDGEMENTS

The work of the second author was supported by NSF grants CME-80-06687 and MEA-83-00158 at the University of Michigan. The first author was supported by a Fellowship from the Ministry of Education, The Peoples' Republic of China. This support is gratefully acknowledged.

NOMENCLATURE

a = total thickness of webs, cm
a_r = cross-sectional area of ride ring, cm^2
b = total width of inner rims, cm
b_r = width of outer rim, cm
c_1 = distance between centroid and inner surface, cm
c_2 = distance between centroid and outer surface, cm
d_1 = thickness of inner rim, cm
d_2 = thickness of outer rim, cm
D_p = inner diameter of ride ring, cm
d_r = outer diameter of ride ring, cm
D_t = diameter of suuport roller, cm
E = modulus of elasticity, kPa
e = ellipticity of ride ring after deformation, cm
e_W = allowable ellipticity of ride ring, cm
g = specific gravity of ride ring, N/cm^3
G_r = weight of ride ring, N
h = cross-sectionl height of ride ring, cm
h_1 = difference of c_1-d_1, cm
h_2 = difference of c_2-d_2, cm
i_r = moment of inertia of cross-sectional area of ri
M_{max} = maximum cross-sectional bending moment of ride
N = number of ribs
Q = load transmitted by ride ring, N
r = diameter ratio of dr to Dt
r_c = radius of centroid circle of cross-sectional area of ride ring, cm
w = section modulus of ride ring, cm^3
σ_B = bending stress of ride ring, kPa
σ_{BW} = working bending stress, kPa
σ_H = contact stress between roller and ride ring, kPa
σ_{HW} = working contact stress, kPa

References

1. B. Saxer,"Estimating the Fatigue Strength of Rotary Kiln Tyres," Zement-Kalk-Gips, (33. Jahrgang) Nr. 6, 1980, pp. 314-316 (in German).

2. W. Bonn and B. Saxer,"Shelltest Measurements on Large Rotary Kilns," Zement-Kalk-Gips, (29. Jahrgang) Nr. 7, 1976, pp. 329-332 (in German).

3. E. Steinbiss,"Investigations on the Mechanical and Thermal Loading of Refractory Bricks in Rotary Cement Kilns," Zement-Kalk-Gips, (30. Jahrgang) Nr. 12, 1977, pp. 625-627 (in German).

4. H. Erni, B. Saxer and F. Schneider,"Deformation of Rotary Kilns and Their Effect on Lining Life," Zement-Kalks-Gips, (32. Jahrgang) Nr. 5, 1979, pp. 236-243 (in German).

5. V. Ramamurti and K. Ragantha Sai, "Deformation and Stresses in Kilns," Zement-Kalk Gips, (31. Jahrgang) Nr. 9, 1978, pp. 433-435.

6. V. Ramamurti and L. S. Gupta, "Design of Rotary Kiln Tyres," Zement-Kalks-Gips, (31. Jahrgang), Nr. 12, 1978, pp. 614-618.

7. K. Mizoguchi, K. Hoshino, K. Shirakawa, Y. Tanigama and N. Otani, "Theoritical and Experimental Researches on Strength of a Rotary Kiln," Bulletin of the Japan Society of Mechanical Engineers, Vol. 23, No. 185, Nov. 1980, pp. 1752-1762.

8. K. Mizoguchi, K. Hoshino, Y. Tanigawa and N. Otani, "Theoretical and Experiment Researches on Strength of a Rotary Kiln," Transactions of the Japan Society of Mechanical Engineers,Vol. 46, No. 403-A, Mar. 1980, pp. 345-354 (in Japanese).

9. R. Clark, "Utility of Insulating Firebrick in Rotary Cement Kilns, A Status Report," Industrial Heating, Vol. 46, No. 4, April 1979, pp. 22-23, 41.

10. H. L. Li, Rotary Kilns: Design, Management and Maintenance, Metallurgical Industry Publishing House, Peking, 1978 (in Chinese).

11. M. Geryk, "Strength Reliability of Revolving Kilns," Czechoslovak Heavy Industry, No. 1, Jan. 1982, pp. 2-12

12. D.J. Wilde, Globally Optimal Design, Wiley-Interscience, New York, 1978

13. P. Papalambros and D.J. Wilde, "Global Non-Iterative Design Optimization Using Monotonicity Analysis," Trans. ASME, Journal of Mechanical Design, Vol. 101, No. 4, 1979, pp. 643-649.

14. P. Papalambros and D.J. Wilde, "Regional Monotonicity in Optimum Design, "Trans. AMSE,Journal of Mechanical Design, Vol. 102, No. 3, 1980, pp. 497-500.

15. P. Papalambros, "Monotonicity in Goal and Geometric Programming," Trans. ASME, Journal of Mechanical Design, Vol. 104, No. 1, 1982, pp. 108-113.

16. P. Papalambros and H.L. Li, "Notes on the Operational Utility of Monotonicity in Optimization," Trans. ASME, Journal of Mechanisms, Transmissions and Automation in Design, Vol. 105, No. 2, 1983, pp. 174-181.

17. P. Papalambros, "Qualitative Monotonicity Analysis of a Problem Involving Differential Equations", Engineering Optimization, Vol. 6, 1983, pp. 117-128.

18. J. Zhou and R. W. Mayne, "Interactive Computing in the Application of Monotonicity Analysis to Design Optimization", Trans. ASME, Journal of Mechanisms, Transmissions and Automation in Design, Vol, 105, No. 2, 1983, pp. 181-187.

19. S. Azarm and P. Papalambros, "An Automated Procedure for Local Monotonicity Analysis", ASME Paper No. 83-DET-48, New York, 1983. Also to appear in Trans. ASME, Journal of Mechanisms, Transmissions and Automation in Design.

20. S. Timoshenko, Strength of Materials, Part 2: Advanced Theory and Problems, 3rd ed., Van Nostrand Reinhold Company, New York, 1970.

21. J.R. Barber, "The Effect of Thermal Distortion on Con-Striction Resistance," International Journal of Heat and Mass Transfer, Vol. 14, 1971, pp. 751-766.

22. J.R. Barber, "Indentation of the Semi-Infinite Elastic Solid by a Hot Sphere," International Journal of Mechanical Sciences, Vol. 15, 1973, pp. 813-819.

List of Figures

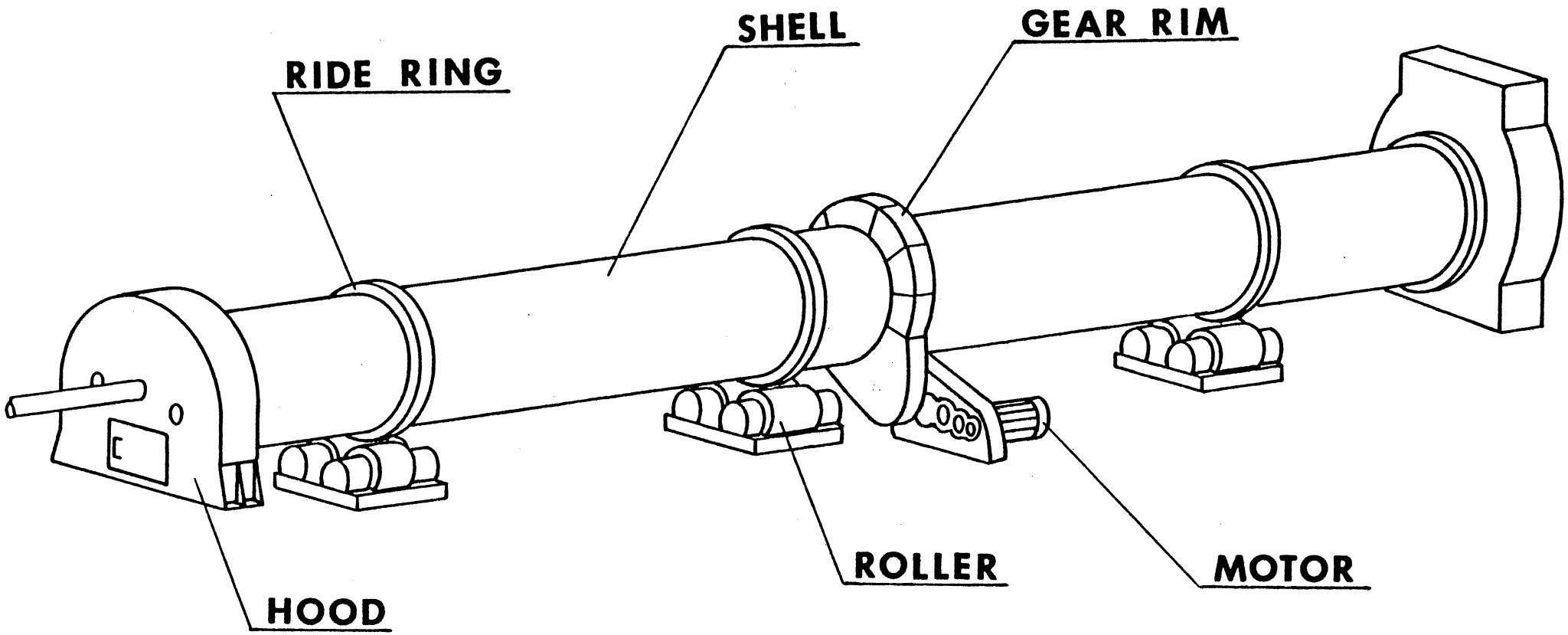

Figure 1

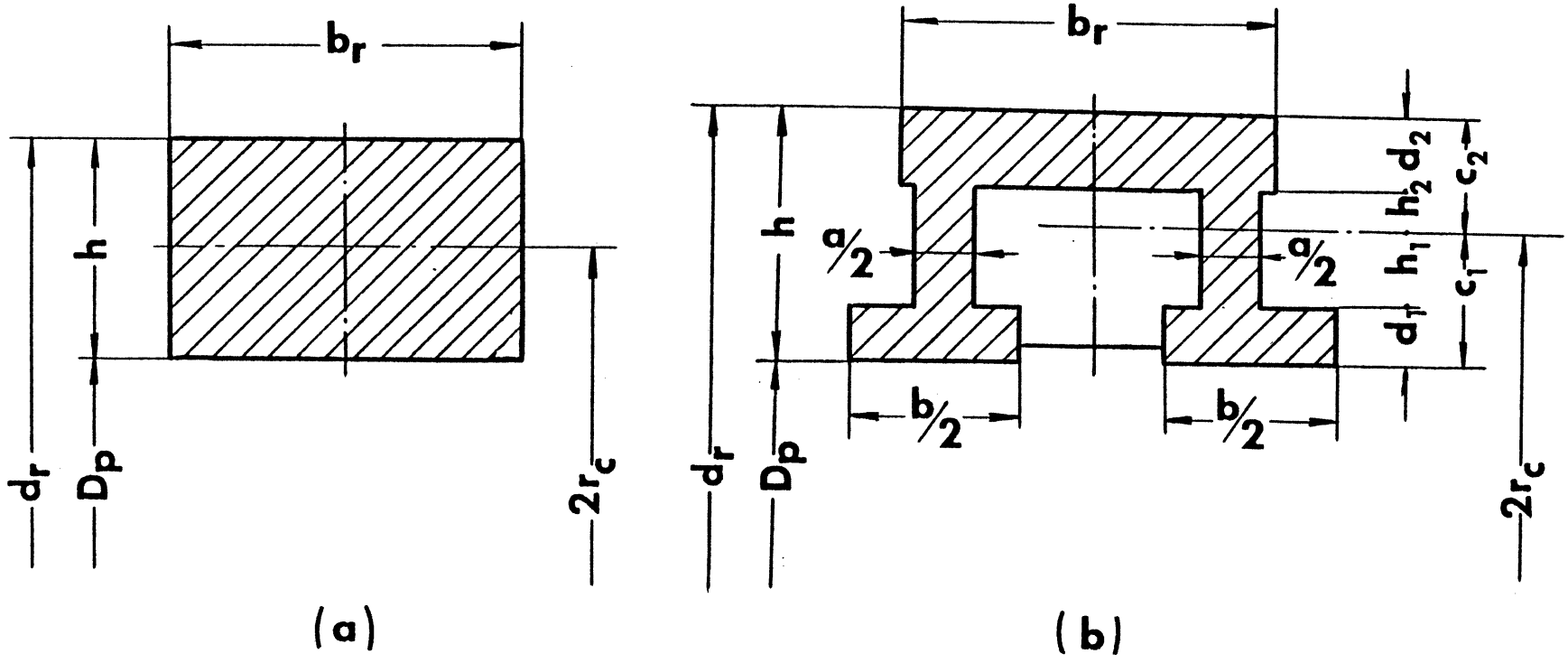

Figure 2

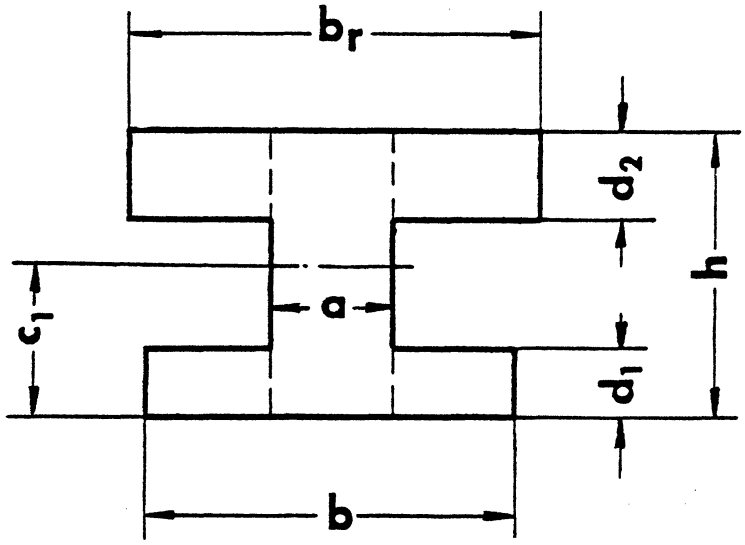

Figure 3

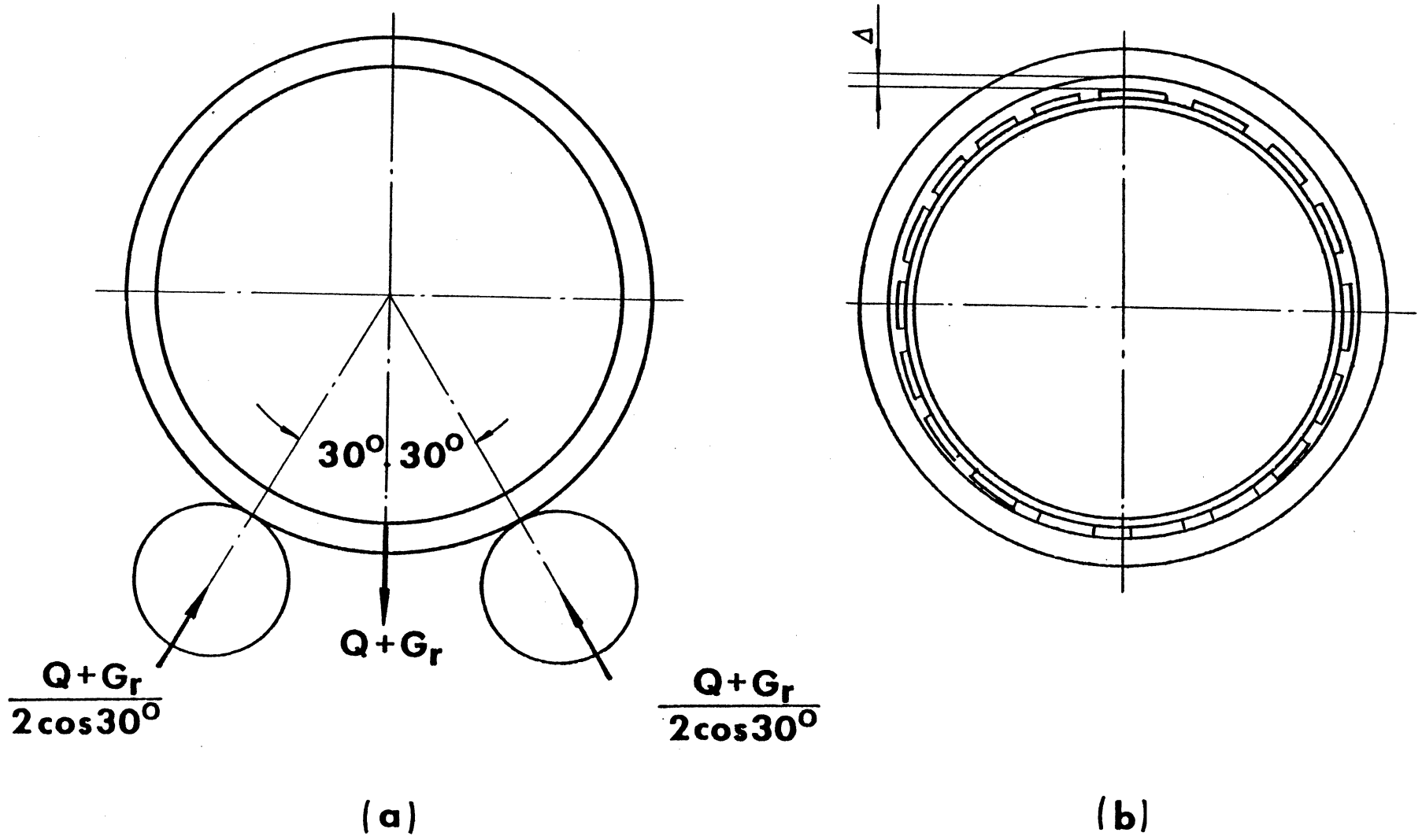

Figure 4

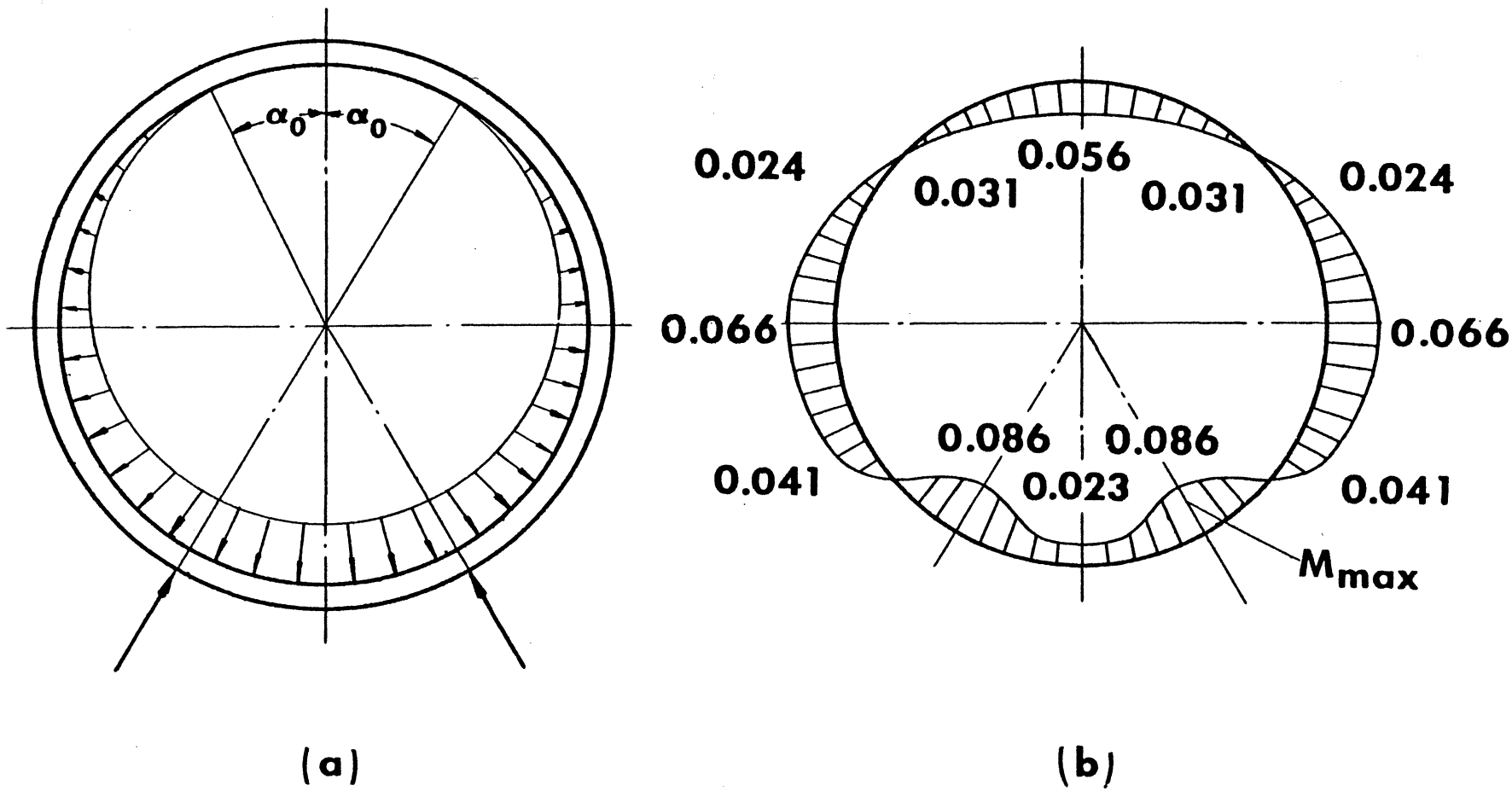
α_0
α_0
0.024
0.056
0.031
0.031
0.024
0.066
0.066
0.086
0.086
0.041
0.023
0.041
M_{max}
(a)
(b)

Figure 5

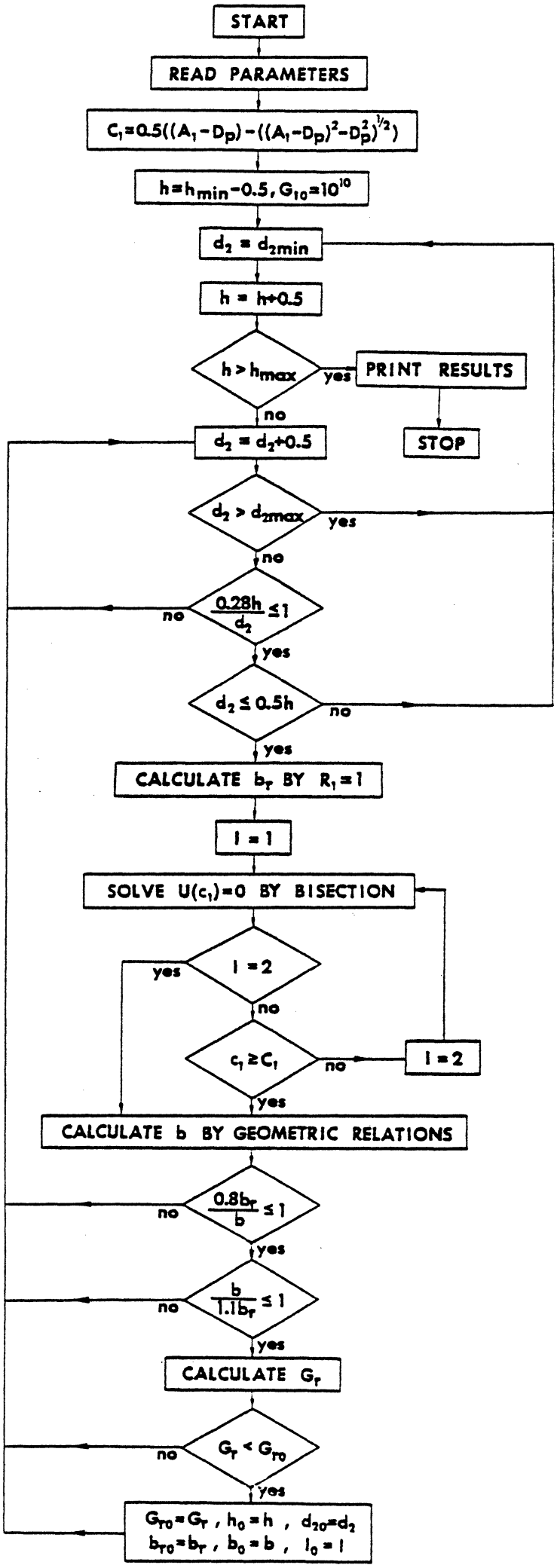
START
READ PARAMETERS
$C_1=0.5((A_1-D_p)-((A_1-D_p)^2-D_p^2)^{1/2})$
$h=h_{min}-0.5, G_{10}=10^{10}$
$d_2 = d_{2min}$
$h = h+0.5$
$h > h_{max}$
yes
PRINT RESULTS
STOP
no
$d_2 = d_2+0.5$
$d_2 > d_{2max}$
yes
no
$\frac{0.28h}{d_2} \leq 1$
no
yes
$d_2 \leq 0.5h$
no
yes
CALCULATE b_r BY $R_1=1$
$l = 1$
SOLVE $U(c_1)=0$ BY BISECTION
$l = 2$
yes
no
$c_1 \geq C_1$
no
$l = 2$
yes
CALCULATE b BY GEOMETRIC RELATIONS
$\frac{0.8b_r}{b} \leq 1$
no
yes
$\frac{b}{1.1b_r} \leq 1$
no
yes
CALCULATE G_r
$G_r < G_{r0}$
no
yes
$G_{r0}=G_r$, $h_0=h$, $d_{20}=d_2$
$b_{r0}=b_r$, $b_0=b$, $l_0=l$

Figure 6

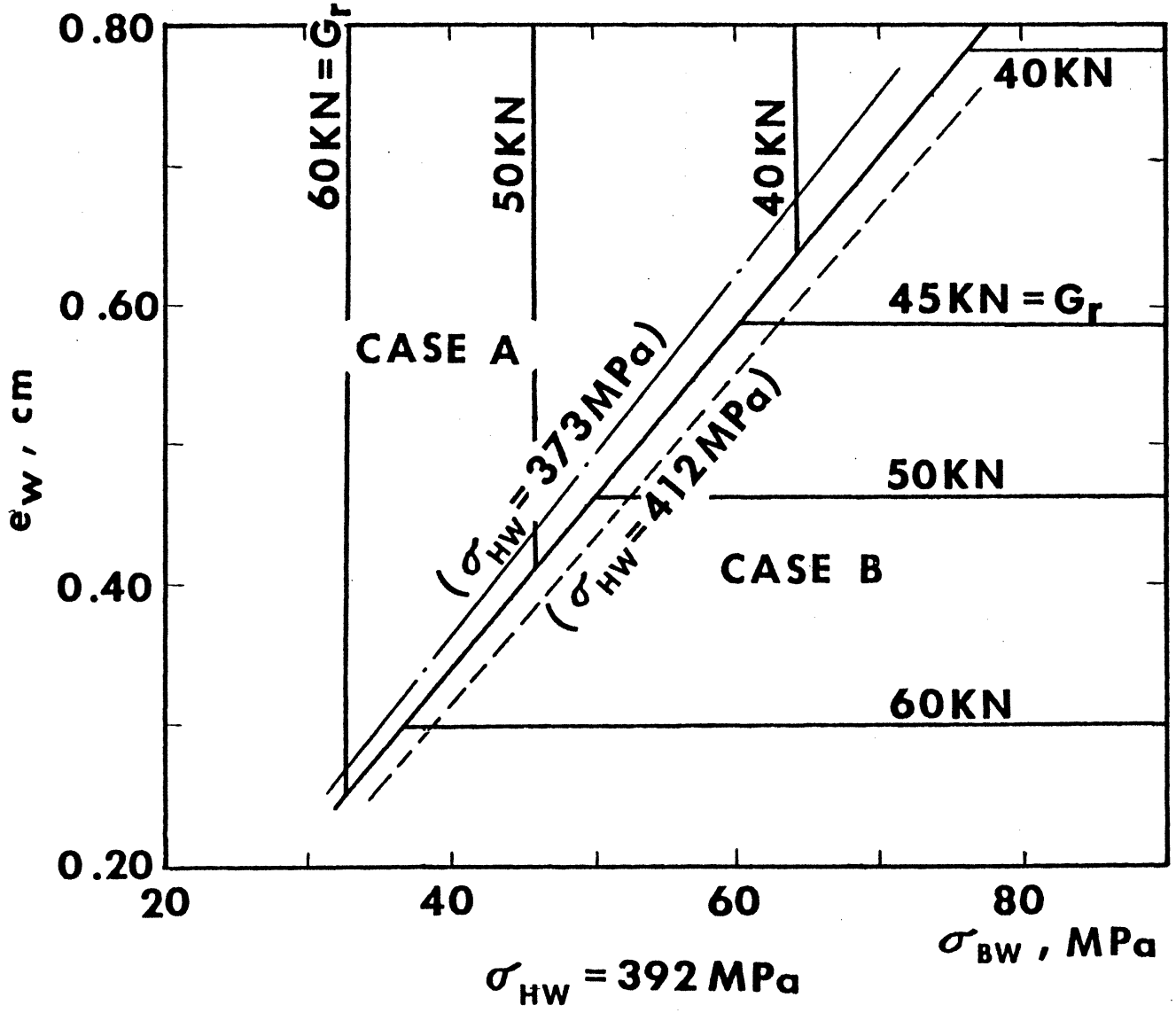
0.80
0.60
0.40
0.20
e_w, cm
20
40
60
80
σ_{BW}, MPa
σ_{HW} = 392 MPa
60KN = G_r
50KN
40KN
40KN
45KN = G_r
50KN
60KN
CASE A
CASE B
(σ_{HW} = 373MPa)
(σ_{HW} = 412MPa)

Figure 7

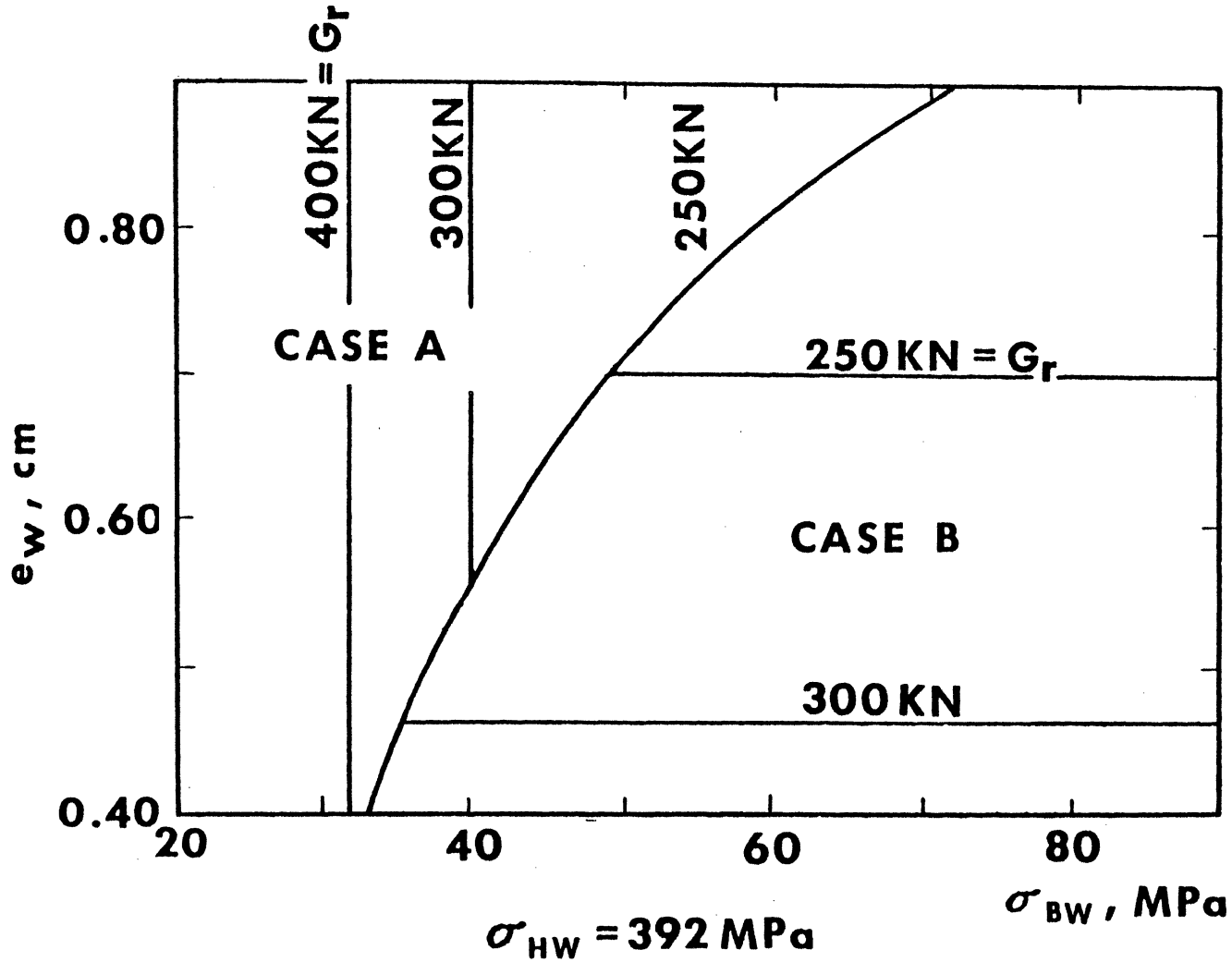
400KN = Gr
300KN
250KN
0.80
0.60
0.40
CASE A
250KN = Gr
CASE B
300KN
20
40
60
80
ew, cm
σBW, MPa
σHW = 392 MPa

Figure 8